Comparative 2D NMR Studies of Human Insulin and Des-pentapeptide Insulin: Sequential Resonance Assignment and Implications for Protein Dynamics and Receptor Recognition†

Qingxin Hua‡,§ and Michael A. Weiss*,‡,∥

Department of Biological Chemistry and Molecular Pharmacology, Harvard Medical School, Boston, Massachusetts 02115, and Department of Medicine, Massachusetts General Hospital, Boston, Massachusetts 02114

Received January 8, 1991; Revised Manuscript Received February 27, 1991

ABSTRACT: The solution structure and dynamics of human insulin are investigated by 2D ^{1}H NMR spectroscopy in reference to a previously analyzed analogue, des-pentapeptide(B26–B30) insulin (DPI; Hua, Q. X., & Weiss, M. A. (1990) *Biochemistry 29*, 10545–10555). This spectroscopic comparison is of interest since (i) the structure of the C-terminal region of the B-chain has not been determined in the monomeric state and (ii) the role of this region in binding to the insulin receptor has been the subject of long-standing speculation. The present NMR studies are conducted in the presence of an organic cosolvent (20% acetic acid), under which conditions both proteins are monomeric and stably folded. Complete sequential assignment of human insulin is obtained and leads to the following conclusions. (1) The secondary structure of the insulin monomer (three α-helices and B-chain β-turn) is similar to that observed in the 2-Zn crystal state. (2) The folding of DPI is essentially the same as the corresponding portion of intact insulin, in accord with the similarities between their respective crystal structures. However, differences between insulin and DPI are observed in the extent of conformational broadening of amide resonances, indicating that the presence or absence of residues B26–B30 influences the overall dynamics of the protein on the millisecond time scale. (3) Residues B24–B28 adopt an extended configuration in the monomer and pack against the hydrophobic core as in crystallographic dimers; residues B29 and B30 are largely disordered. This configuration differs from that described in a more organic milieu (35% acetonitrile; Kline, A. D., & Justice, R. M., Jr. (1990) *Biochemistry 29*, 2906–2913), suggesting that the conformation of insulin in the latter study may have been influenced by solvent composition. (4) The insulin fold is shown to provide a model for collective motions in a protein with implications for the mechanism of protein–protein recognition. To our knowledge, this paper describes the first detailed analysis of a protein NMR spectrum under conditions of extensive conformational broadening. Such an analysis is made possible in the present case by comparative study of an analogue (DPI) with more tractable spectroscopic properties.

Insulin provides a model for biophysical studies of protein structure and dynamics and has been extensively investigated by X-ray crystallography (Blundell et al., 1971; Peking Insulin Structure Group, 1971; Bi et al., 1984; Smith et al., 1984; Dai et al., 1987; Baker et al., 1988), thermal diffuse X-ray scattering (Caspar et al., 1988) and molecular dynamics simulations (Kruger et al., 1987; Caves et al., 1990). The insulin fold is highly conserved among vertebrate and invertebrate kingdoms, defining an ancestral family of insulin-like proteins (Blundell & Humbel, 1980). Interest in this family has been stimulated by the identification of a related class of tyrosine kinase linked receptors involved in cellular regulation and development. Mutations in insulin have been identified in association with diabetes mellitus (Haneda et al., 1984) and in the insulin receptor in association with clinical syndromes of insulin resistance and developmental abnormalities (Taira et al., 1989; Odawara et al., 1989).

Insulin is composed of two polypeptide chains, an A-chain of 21 residues and B-chain of 30 residues. Despite their small size, these chains contain representative elements of secondary structure, tertiary organization, and disulfide bonding generally observed in larger systems (Figure 1; Baker et al., 1988). Differences in the conformation of insulin protomers are observed among crystal forms and have been regarded as a model for the transmission of conformational change (Chothia et al., 1983). The structure and flexibility of the insulin monomer have been the subject of considerable speculation in relation to the mechanism of receptor recognition (Baker et al., 1988; Mirmira & Tager, 1989). The present NMR experiments are conducted under monomeric conditions (20% acetic acid) as previously described (Weiss et al., 1989). Control experiments demonstrate that insulin adopts a native conformation under these conditions; in particular, ^{1}H NMR spectra of human proinsulin (Weiss et al., 1990) and des-pentapeptide insulin (Boelens et al., 1990; Hua & Weiss, 1990) are similar in the absence and presence of 0–20% acetic acid.

The ^{1}H NMR spectrum of insulin ordinarily exhibits extensive variation in the line widths of amide resonances. Such variation is related to exchange among conformational substates (Weiss et al., 1989; Kline & Justice, 1990) and has also been observed in an engineered insulin monomer in aqueous solution (Weiss et al., 1991). Although of interest in relation to insulin dynamics (Kruger et al., 1987; Caspar et al., 1988; Caves et al., 1990), exchange-mediated line-broadening limits

† This work was supported in part by grants from the National Institutes of Health, American Diabetes Association, and Juvenile Diabetes Foundation International to M.A.W. M.A.W. is supported by the Pfizer Scholars Program for New Faculty and the American Cancer Society.

* Address correspondence to this author at the Department of Biological Chemistry and Molecular Pharmacology, Harvard Medical School.

‡ Harvard Medical School.

§ Permanent address: Institute of Biophysics, Academia Sinica, Beijing, China.

∥ Massachusetts General Hospital.

0006-2960/91/0430-5505$02.50/0

the straightforward application of sequential ^1H NMR assignment methods (Weiss et al., 1989). In the present study, this limitation is overcome by comparative analysis of the 2D NMR spectra of insulin and a truncated analogue, des-pentapeptide(B26–B30) insulin (DPI;[1] lacking the C-terminal five residues of the B-chain). Although the spectra of the two proteins are very similar, that of the DPI exhibits markedly less resonance broadening (presumably due to more rapid motions in the fragment), and a detailed analysis of its 2D NMR spectra has recently been described (Boelens et al., 1990; Hua & Weiss, 1990). Comparative analysis of insulin and DPI permits the corresponding assignment of the intact protein and provides information regarding the environments of residues B26–B30 in an insulin monomer. The observed NMR features suggest the existence of collective motions of α-helices on the millisecond time scale.

Materials and Methods

Biosynthetic human insulin and DPI were provided by Eli Lilly & Co. (Indianapolis, IN) and prepared as described (Weiss et al., 1989). Spectra were acquired at 25 °C in 80% H_2O/20% deuterated acetic acid or 80% D_2O/20% deuterated acetic acid as described (Hua & Weiss, 1990). Two-dimensional experiments were performed by the pure-phase method of States et al. (1982) at 500 MHz (Harvard Medical School NMR Center) and ordinarily acquired with 4K points in the t_2 dimension and 600 t_1 increments. Data were zero-filled to 4K in the t_1 dimension; exponential and shifted sine-bell window functions were applied in both dimensions prior to Fourier transformation.

Results

Structural Overview and Rationale: The structure of the insulin monomer has not been directly determined either in the crystal state or in solution. A model of the insulin monomer may be inferred, however, from the structure of crystallographic protomers (Baker et al., 1988), as shown in schematic form in panel A of Figure 1. The A-chain consists of N- and C-terminal α-helices (residues A1–A8 and A13–A19; A20 and A21 are extended); the B-chain consists of an N-terminal region of variable configuration, a central α-helix (residues B9–B19), a $\beta(1\rightarrow4)$-turn (residues B20–B23), and a C-terminal β-strand (residues B24–B28; B29 and B30 have variable configuration).

Insulin's conformation in the crystal state is influenced by subunit interactions, especially in the C-terminal β-strand of the B-chain. This region forms an antiparallel β-sheet in the dimer interface, which is stabilized by an extensive set of van der Waal's interactions between protomers (Baker et al., 1988). Despite the importance of this region in receptor binding (Pullen et al., 1976; Dodson et al., 1979; Baker et al., 1988; Mirmira & Tager, 1989), its structure in the absence of dimerization has not been determined. Insulin's major structural features are otherwise retained in the crystal structure of a truncated monomeric analogue, des-pentapeptide(B26–B30) insulin (DPI; see panel B of Figure 1) (Bi et al., 1984; Dai et al., 1987), which therefore provides an appropriate model of the insulin core.

We have previously described the sequential assignment of DPI (Hua & Weiss, 1990) and now seek to extend these results to intact insulin. Our results support a simple model in which

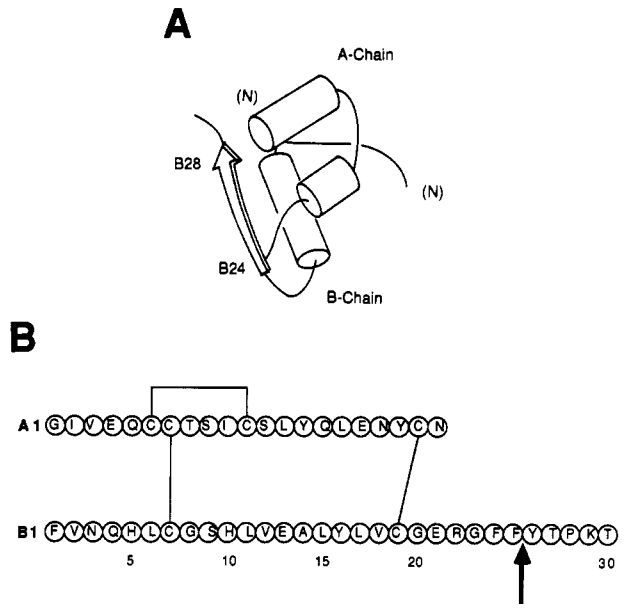

FIGURE 1: (A) Cylinder (α-helix) and arrow (β-strand) representation of the crystal structure of human insulin (2-Zn form; Blundell et al., 1971; Peking Insulin Structure Group, 1971). The positions of residues B24 and B28 are indicated. (B) The primary structure of human insulin is shown in single-letter code. The arrow indicates the chymotryptic-sensitive site (PheB25↓TyrB26) used to generate DPI. The positions of the three disulfide bonds are indicated.

insulin consists of a stably folded moiety (DPI) with C-terminal extension (residues B24–B28) that packs as a β-strand against the hydrophobic core (panel A of Figure 1). Flexibility of this structure is suggested by the absence of some (but not all) interchain NOEs predicted by crystal models; these NOEs are presumably quenched by subnanosecond fluctuations in interproton vectors. The NMR features also suggest the presence of collective low-frequency modes that involve the relative displacement of structural elements on a millisecond time scale.

Spin System Identification and Comparative Assignment: The primary structure of human insulin (51 residues) is shown in panel B of Figure 1; it differs from DPI by the presence of the five additional spin systems belonging to TyrB26, ThrB27, ProB28, LysB29, and ThrB30 (arrow in Panel B). A unique 2D NMR spin system is observed for each residue under the conditions of study, consistent with the presence of a well-defined oligomeric state (the monomer). As expected, additional spin systems characteristic of proline (B28), lysine (B29), and two threonines (B27 and B30) are observed in the TOCSY spectrum of insulin (panel A of Figure 2) relative to the corresponding spectrum of DPI (panel B). The remaining NMR spin systems shown in Figure 2 exhibit similar chemical shifts in the two spectra; their assignments are as indicated and in selected cases described below. The expected B26 tyrosine-specific aromatic and α–β_1–β_2 spin systems are observed elsewhere in the spectrum (Table I; data not shown). As illustrated in the spectral region shown in Figure 2, there is a detailed similarity between the chemical shifts of corresponding protons in insulin and DPI, suggesting that the structural similarity apparent in their crystal structures (Bi et al., 1984; Dai et al., 1987) is maintained in solution. The majority of resonances exhibit nearly identical chemical shifts (±0.03 ppm); differences greater than 0.1 ppm are observed only for seven spin systems: GlyA1, GlnA15, TyrA19, CysA20, GluB21, PheB24, and PheB25. These perturbations presumably reflect structural or magnetic effects of the additional residues B26–B30. Assignments of corresponding spin systems in the two spectra are verified by sequential methods

[1] Abbreviations: DPI, des-pentapeptide(B26–B30) insulin; HI, human insulin; NOE, nuclear Overhauser enhancement; NOESY, 2D NOE spectroscopy; photo-CIDNP, photochemically induced dynamic nuclear polarization; TOCSY, 2D isotropic mixing (Hartman–Hahn) spectroscopy; DQF-COSY, double-quantum-filtered 2D correlation spectroscopy.

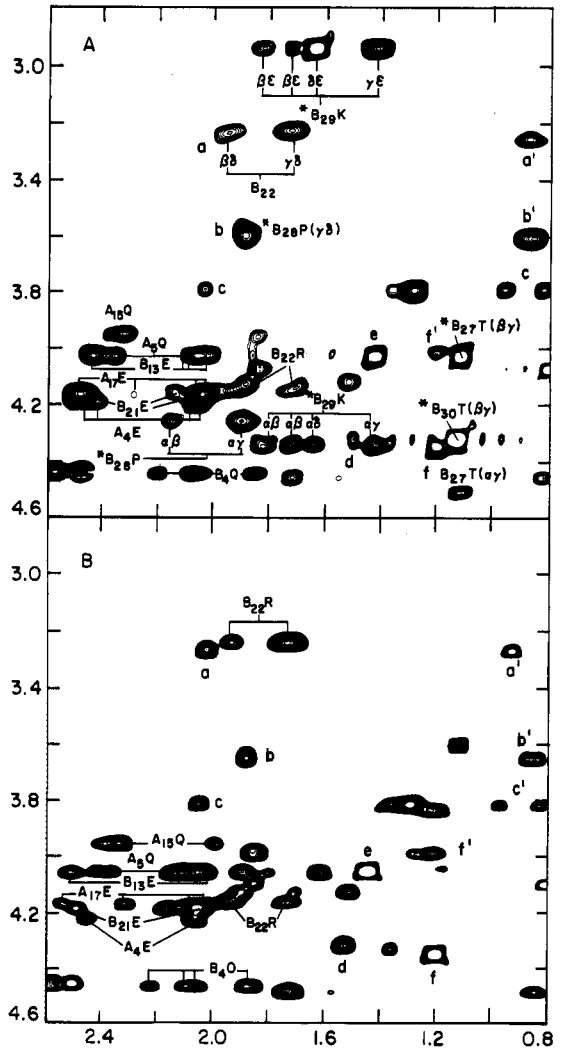

FIGURE 2: Identification of additional aliphatic NMR spin systems due to ThrB27–ProB28–LysB29–ThrB30 evident in the TOCSY spectrum of human insulin (panel A; asterisks) relative to corresponding spectrum of DPI (panel B). The aromatic and AMX spin systems of TyrB26 are observed in other regions of the spectrum and have been described previously (Weiss et al., 1989). The remaining resonances in this region exhibit similar chemical shifts in the two spectra. The spin systems of GluA4, GlnA5, GlnA15, GluA17, GlnB4, GluB13, GluB21, and ArgB22 are labeled in standard single-letter code (see Table I); additional cross-peaks are assigned as follows: a (B12 α–β), a′ (B12 α–γ), b (A3 α–β), b′ (A3 α–γ1 and α–γ2), c (B18 α–β), c′ (B18 α–γ1 and α–γ2), d (A10 α–β), e (B14 α–β), f (A8 β–γ), and f′ (A8 α–γ). The mixing time was 55 ms. Axes are labeled in parts per million relative to acetic acid (2.03 ppm).

(Wuthrich et al., 1983). The ^{1}H NMR assignments[2] of human insulin in 20% acetic acid are summarized in Table I. Stereospecific assignment of β resonances is obtained for selected residues by the method of Wagner et al. (1987); these are indicated by asterisks in Table I and given in Table S1 (in supplementary material). Differences in chemical shift relative to DPI are given in Table S2. We note in passing that there are more substantial differences in chemical shifts relative to the results of Kline and Justice (1990); these differences are likely to arise from differences in solvent conditions and are considered further in Table S3 and in the Discussion.

Sequence-Specific Assignment and Conformational Broadening: Sequential assignment of the A- and B-chains of human insulin is analogous to that described for DPI (Hua & Weiss, 1990) and will not be repeated here in detail. As suggested by the 1D ^{1}H NMR spectra previously published (Weiss et al., 1989; Hua & Weiss, 1990), more extensive exchange-related broadening of amide resonances is observed in the 2D "fingerprint" region of insulin than in that of DPI (Figure 4). Short-range and medium-range contacts are summarized in schematic form in Figure 3. Residues B24–B30 exhibit the strong $d_{\alpha N}$/weak d_{NN} connectivity pattern that

Table I: Chemical Shift of the Assigned ^{1}H NMR Resonances[a] of Human Insulin (20% Deuterated Acetic Acid and 25 °C)

	chemical shifts at 25 °C			
residue	NH	CαH	CβH	others
A1 Gly		4.11, 3.58		
A2 Ile	8.48	3.91	1.16	$C\gamma H_2$ 1.16, 0.94 $C\gamma H_3$ 0.72; $C\delta H_3$ 0.58
A3 Val	8.10	3.60	1.88	$C\gamma H_3$ 0.88, 0.84
A4 Glu	8.10	4.19	2.03, 2.03	$C\gamma H_2$ 2.41, 2.47
A5 Gln	8.25	4.04	2.08,* 2.03*	$C\gamma H_2$ 2.44, 2.36 $N\epsilon H_2$ 6.84, 7.46
A6 Cys	8.26	4.86	2.85,* 3.32*	
A7 Cys	8.22	4.80	3.73,* 3.27*	
A8 Thr	8.17	4.03	4.35	$C\gamma H_3$ 1.20
A9 Ser	7.39	4.73	4.02, 3.85	
A10 Ile	7.78	4.32	1.53	$C\gamma H_2$ 1.05, 0.39 $C\gamma H_3$ 0.60; $C\delta H_3$ 0.45
A11 Cys	9.62	4.86	3.13, 2.84	
A12 Ser	8.70	4.55	3.95,* 4.25*	
A13 Leu	8.57	3.80	1.37, 1.30	$C\gamma H$ 1.37; $C\delta H_3$ 0.74, 0.69
A14 Tyr	7.43	4.12	2.95,* 2.85*	C2, 6 H 7.00; C3, 5 H 6.78
A15 Gln	7.50	3.95	2.34, 1.99	$C\gamma H_2$ 2.40; $N\epsilon H_2$ 7.01, 7.44
A16 Leu	8.02	4.12	1.88, 1.52	$C\gamma H$ 1.70; $C\delta H_3$ 0.78, 0.74
A17 Glu	8.00	4.16	2.08, 2.03	$C\gamma H_2$ 2.53, 2.28
A18 Asn	7.38	4.44	2.57, 2.50	$N\delta H_2$ 6.50, 7.12
A19 Tyr	7.86	4.44	2.93,* 3.30*	C2, 6 H 7.28; C3, 5 H 6.72
A20 Cys	7.38	4.73	3.22, 2.80	
A21 Asn	8.16	4.68	2.82, 2.70	$N\delta H_2$ 7.45, 6.61
B1 Phe		4.22	3.11, 3.11	C2, 6 H 7.16; C3, 5 H 7.30 C4H 7.23
B2 Val	8.08	4.08	1.85	$C\gamma H_3$ 0.79, 0.79
B3 Asn	8.43	4.67	2.67, 2.67	$N\delta H_2$ 7.48, 6.86
B4 Gln	8.35	4.44	2.05,* 1.87*	$C\gamma H_2$ 2.21, 2.21 $N\epsilon H_2$ 7.29, 6.74
B5 His	8.58	4.44	3.20,* 3.51*	C2H 8.54; C4H 7.34
B6 Leu	8.93	4.47	1.72,* 0.84*	$C\gamma H$ 1.56; $C\delta H_3$ 0.84, 0.68
B7 Cys	8.30	4.95	3.17, 2.91	
B8 Gly	9.22	3.96, 3.81		
B9 Ser	9.02	4.08	3.84, 3.84	
B10 His	7.96	4.47	3.52,* 3.28*	C2H 8.66; C4H 7.43
B11 Leu	7.05	3.96	1.84,* 1.24*	$C\gamma H$ 1.26; $C\delta H_3$ 0.74, 0.69
B12 Val	7.12	3.28	1.99	$C\gamma H_3$ 0.88, 0.88
B13 Glu	7.87	4.04	2.11, 2.03	$C\gamma H_2$ 2.49
B14 Ala	7.68	4.04		$C\beta H_3$ 1.44
B15 Leu	8.00	3.82	1.28	$C\gamma H$ 1.41; $C\delta H_3$ 0.62, 0.43
B16 Tyr	8.06	4.22	3.08, 3.08	C2, 6 H 7.06; C3, 5 H 6.72
B17 Leu	7.78	4.04	1.60,* 1.87*	$C\gamma H$ 1.80, $C\delta H_3$ 0.87, 0.87
B18 Val	8.48	3.80	2.04	$C\gamma H_3$ 0.96, 0.83
B19 Cys	8.67	4.73	2.88,* 3.22*	
B20 Gly	7.68	3.90, 3.90		
B21 Glu	8.36	4.18	2.14, 2.04	$C\gamma H_2$ 2.48, 2.48
B22 Arg	7.94	4.17	1.92, 1.92	$C\gamma H_2$ 1.72, 1.72 $C\delta H_2$ 3.22, 3.22; $N\epsilon H$ 7.10
B23 Gly	7.64	3.90, 3.79		
B24 Phe	8.11	4.19	3.15*, 3.08*	C2, 6 H 6.90; C3, 5 H 7.04
B25 Phe	8.20	4.63	3.06, 2.97	C2, 6 H 7.14; C3, 5 H 7.22 C4H 7.18
B26 Tyr	7.92	4.58	2.86, 2.86	C2, 6 H 6.93; C3, 5 H 6.70
B27 Thr	7.75	4.51	4.04	$C\gamma H_3$ 1.13
B28 Pro		4.28	2.17, 2.17	$C\gamma H_2$ 1.89, 1.89 $C\delta H_2$ 3.60, 3.53
B29 Lys	8.17	4.34	1.83, 1.72	$C\gamma H_2$ 1.42, 1.42 $C\delta H_2$ 1.64, 1.64 $C\epsilon H_2$ 3.60, 3.53 $N\epsilon H_2$ 7.43, 7.43
B30 Thr	7.95	4.33	4.33	$C\gamma H_3$ 1.13

[a] Chemical shifts are measured relative to the residual CH_3 resonance of acetic acid, presumed to be 2.03 ppm. Selected stereospecific assignments of β resonances were obtained by the method of Wagner et al. (1987) and are indicated by asterisks.

[2] Nomenclature: stereospecific assignments of β protons (asterisks in Table I) are designated β_2 and β_3 in accord with Wuthrich (1987); resonances are otherwise designated 1 (downfield) or 2 (upfield), i.e., β_1 and β_2, γ_1 and γ_2, etc.

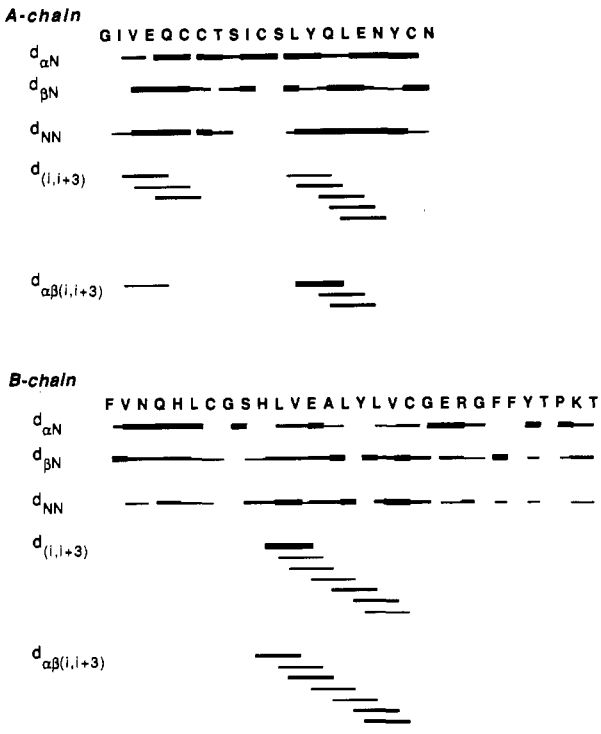

FIGURE 3: Schematic representation of the sequential connectivities in the A-chain (top panel) and B-chain (bottom panel). The primary structure of the two chains are given in one-letter code. Symbols $d_{\alpha N}$, d_{NN}, etc. are as defined by Wuthrich (1986). $d_{(i,i+3)}$ denotes NOEs between the α-proton of residue i and the amide proton of residue $i + 3$. With each class, relative apparent NOE intensity is schematically represented by line thickness. α-helices (A-chain residues 2–8 and 13–18; B-chain residues 9–19) are defined by the pattern of $(i, i + 3)$ NOEs and by continuous strings of d_{NN} connectivities that are stronger in DPI and insulin than those generally observed in nonhelical regions; strong d_{NN} connectivities are also observed in the turn between residues B20–B23.

is characteristic of an extended strand (Wuthrich, 1986); no $(i, i + 3)$ or $(i, i + 4)$ contacts are observed in this region. An additional insulin-specific sequential connectivity (ThrB27H_α to ProB28$H_{\delta 1}$ and -$H_{\delta 2}$) is observed in the NOESY spectrum in D_2O (panel B of Figure 5; asterisk) and is absent as expected in the spectrum of DPI (panel A). These NOEs (and the absence of cis-related B27H_α–B28H_α NOEs) establish the geometry of the B27–B28 peptide bond as trans in accord with crystal models. No minor cross-peaks are observed whose presence would indicate cis–trans isomerization of the ThrB27–ProB28 peptide bond, as previously described for human insulin in 35% acetonitrile (Kline & Justice, 1990). Additional evidence for the stable packing of residues B24–B28 as a β-strand is provided by an $(i, i + 2, i + 4)$ pattern of long-range contacts with the hydrophobic core (see below). The $d_{\alpha N}$ contacts of residues B29 and B30 are weaker than those of residues B24–B28, consistent with increased flexibility of the C-terminal two residues.

Secondary Structure: The presence and location of α-helices in human insulin may be established by observation of characteristic $d_{\alpha N}(i, i + 3)$ and $d_{\alpha\beta}(i, i + 3)$ sequential connectivities and are identical with the corresponding α-helices in DPI (Hua & Weiss, 1990). In both proteins, evidence of stable helix formation is also provided by the presence of corresponding slowly exchanging amide resonances (see below). In each protein the participation of GlyA1 in the N-terminal helix of the A-chain is unclear. The correspondence of α-helical segments in insulin and DPI has previously been inferred from the similarity of their CD spectra (Lu, 1981) and crystal structures (Bi et al., 1984; Dai et al., 1987).

ϕ-Related Coupling Constants: The $^3J_{H_N-H_\alpha}$ coupling constant is related to the backbone dihedral angle ϕ by a Karplus equation (Pardi et al., 1984) and is ordinarily measured by the apparent separation of antiphase multiplets in the fingerprint region of DQF-COSY spectra. The relationship between true and apparent separation is critically influenced by line broadening, however, especially under conditions in which line widths exceed the magnitude of the coupling constants (Neuhaus et al., 1985). This is the case for the majority of residues in DPI and insulin. The apparent antiphase separations for DPI are given in Table S4 and compared to ϕ values obtained from the two asymmetric promoters of the 2-Zn crystal (Baker et al., 1988). As expected, the apparent couplings are consistently larger than what would be predicted by a Karplus-type analysis of crystallographic ϕ values (Pardi et al., 1984). Insulin exhibits a similar pattern of apparent multiplet separations, with the addition of residues B26–B30 (Table S5). Since residues B27–B30 exhibit relatively narrow line widths (boldface in the table), their apparent couplings may be interpreted. That observed for LysB29 (7.8 Hz) is not consistent with continuation of a stable β-strand (expected to be > 8.9 Hz; Pardi et al., 1984). This intermediate value is likely to reflect averaging of multiple configurations in accord with the observed absence of interresidue NOEs. Interestingly, the B30 coupling (9.5 Hz) suggests a nonrandom preference in ϕ values.

Dynamic Implications of Conformational Broadening: Sites of disproportionately broad amide resonances are not localized in one region of the structure, but preferentially involve each of the elements of secondary structure and also the cystine cross-links (Figure 4). This pattern suggests that collective motions *involving all three α-helices and β-turn* are responsible for conformational exchange; this interpretation is in accord with structural transitions observed among crystal structures (Chothia et al., 1983) and the presence of liquid-like motions in the hydrophobic core, as inferred from thermal diffuse X-ray scattering (Caspar et al., 1988). Conversely, the sharper amide resonances belong to regions (loops, turn, and chain termini) whose motions might be expected to be faster or uncorrelated. To understand the physical origins of these line widths, two distinct mechanisms must be considered.

(*i*) *True Motional Narrowing*: The relaxation of disordered side chains, loops, or arms is determined by segmental mobility rather than the overall rotational correlation time of the system. These motions occur on the subnanosecond-to-nanosecond time scale and would be expected for residues lacking significant interresidue contacts. This mechanism appears to be operative for PheB1, ValB2, LysB29, and ThrB30; the ends of long side chains on the protein surface may also be disordered.

(*ii*) *Apparent Narrowing*: Residues A10 and B3–B6 (the "HisB5–IleA2 pocket"), A18–A20 (an interchain contact region), and B27–B28 (β-strand) each exhibit stable packing interactions (see Long-Range NOEs, below) and yet their amide resonances are "narrowed" relative to α-helical residues (Figure 4). Their line widths are appropriate for a small protein, however, indicating that the apparent narrowing is due only to the *absence* of conformational broadening. Presumably, these protons experience a more limited range of chemical shifts ($\Delta\omega$) in the course of the postulated collective modes. The present data do not exclude the presence of additional local motions in these regions (e.g., swinging of the A-chain loop).

Long-Range NOEs: Human insulin in solution contains elements of secondary structure (above) whose relative ori-

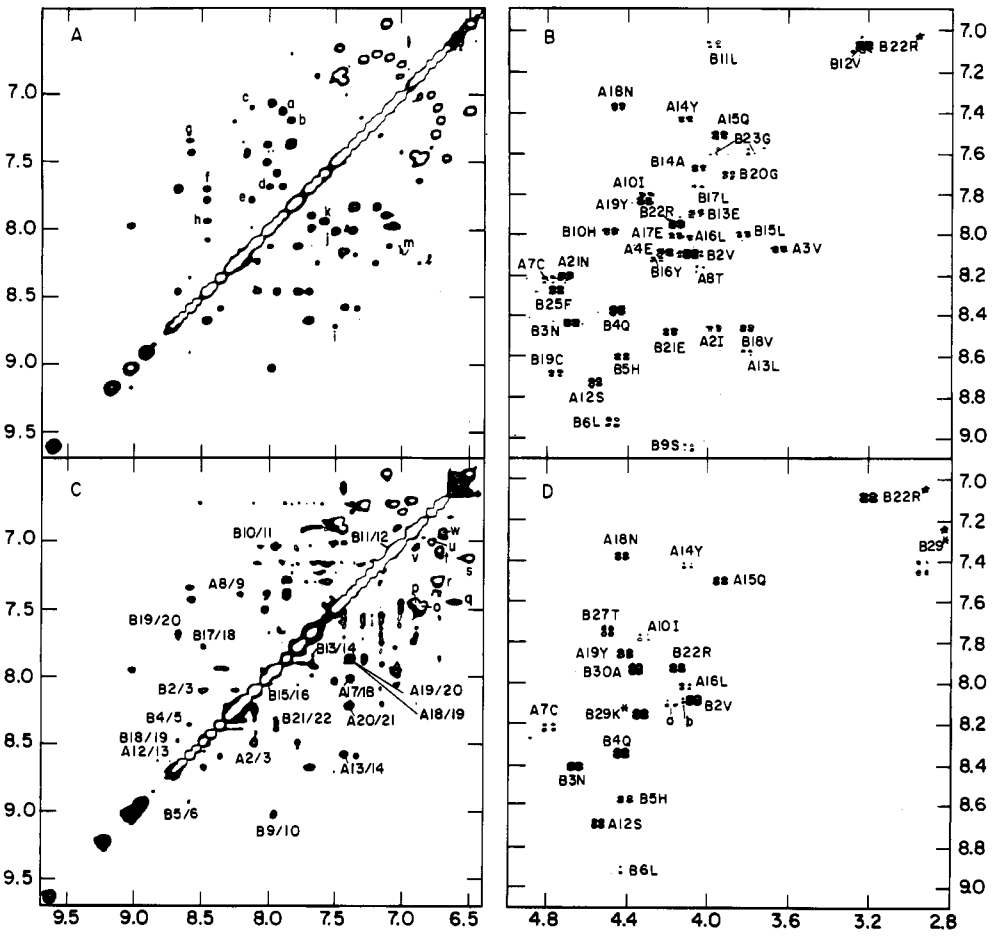

FIGURE 4: Spectrum showing extensive H_N–H_N cross-peaks observed in the NOESY spectrum of DPI (panel A), corresponding to the two A-chain α-helices, central B-chain α-helix, and B-chain β-turn. A portion of these cross-peaks are broadened in the NOESY spectrum of intact insulin (panel C). Related antiphase cancellation of fingerprint H_N–H_α cross-peaks is observed in the DQF-COSY spectra of human insulin (panel D) relative to that of DPI (panel B). The contour levels in each panel were normalized to the ortho–meta cross-peak of TyrA14, which exhibits approximately the same T_2 in both proteins. Assignment of the DPI spectra is as previously described (Hua & Weiss, 1990). Assignments in panel A: (a) B13H_N–B12H_N, (b) A19H_N–A19H_δ, (c) B16H_N–B16H_δ, (d) B15H_N–B14H_N, (e) B17H_N–B16H_N, (f) B21H_N–B20H_N, (g) B5H_N–B5H_δ, (h) B22H_N–B21H_N, (i) A15H_N–A12H_N, (j) A17H_N–A15H_N, (k) B23H_N–B22H_N, (l) B25H_N–B24H_δ, and (m) B16H_N–B24H_ϵ. Assignments in panel C (intraresidue NOEs): (o) A5ϵNH_2 and B3δNH_2, (p) A15ϵNH_2, (q) A21δNH_2, (r) B4ϵNH_2 and A19 ortho/meta, (s) B18γNH_2, (t) B16 ortho/meta, (u) A14 ortho/meta, (v) B24 ortho/meta, and (w) B26 ortho/meta. Assignments in panel D: (a) B16Y and (b) B24F. Asterisks in panels B and D indicate cross-peaks involving side-chain NH or NH_2 resonances.

entation gives rise to long-range NOEs (representative data is shown in Figures 6 and 7). These may be classified according to the type of secondary structure involved (e.g., helix–helix contacts, helix–strand contacts, etc.) and are discussed in turn below.

We note in passing that a significant number of long-range contacts predicted by crystal structures are not observed in solution. The absent NOEs correspond in general to interactions that differ among inequivalent protomers and among different crystal forms. The implications of this observation for protein dynamics and molecular modeling of the solution structure will be discussed in detail elsewhere (manuscript in preparation).

Comparison of long-range NOEs in insulin and DPI indicates that the DPI moiety of insulin has the same structure as DPI itself and that the C-terminal β-strand remains tethered to the hydrophobic core as predicted by crystal structures. The detailed similarity of NOE patterns between insulin and DPI in essence provides an extended control: in contrast, their relative differences in extent of line broadening (above) must have a dynamic rather than structural origin.

(*i*) *Helix–Helix Contacts within the A-Chain*: Packing interactions within the A-chain are observed between TyrA19 and IleA2 (panel A of Figure 6); additional interactions are observed between CysA6 and LeuA16 (data not shown). These interactions are also observed in DPI (panel B) and are in accord with crystal models. The striking conservation of these four residues among insulin sequences—A2 (Ile/Val), A6 (Cys), A16 (Leu, Ile), and A19 (Tyr) (Pullen et al., 1976; Demeyts et al., 1984; Baker et al., 1988)—suggests that these sites contain high informational content (Reidhaar-Olson & Sauer, 1988); i.e., their long-range interaction is likely to be a defining element of the insulin fold.

(*ii*) *Helix Contacts between Chains*: Long-range NOEs between the A-chain and B-chain reflect the relative orientation of the three helices. As predicted by the crystal models, NOEs are observed between the first helix of the A-chain and the N-terminal portion of the B-chain helix (ValA3γ_1CH_3 and B11H_α; IleA2 side chain and B11H_α; IleA2 also exhibits contacts with β-protons of B7 and B8) and between the C-terminal helix of the A-chain and the C-terminal portion of the B-chain helix (TyrA19 meta and B15$_\delta CH_3$ resonances, as shown in Figure 6). Each of these sets of NOEs is essentially the same in the spectra of insulin and DPI (panels A and B, respectively). Long-range contacts are also observed between nonhelical residues AsnA21N_ϵ and B22H_β; interchain NOEs involving the N-terminal region of the B-chain (B1–B6) are described below.

(*iii*) *N-Terminal Region of B-Chain*: In the crystal, residues B1–B8 ordinarily adopt an extended conformation (the T

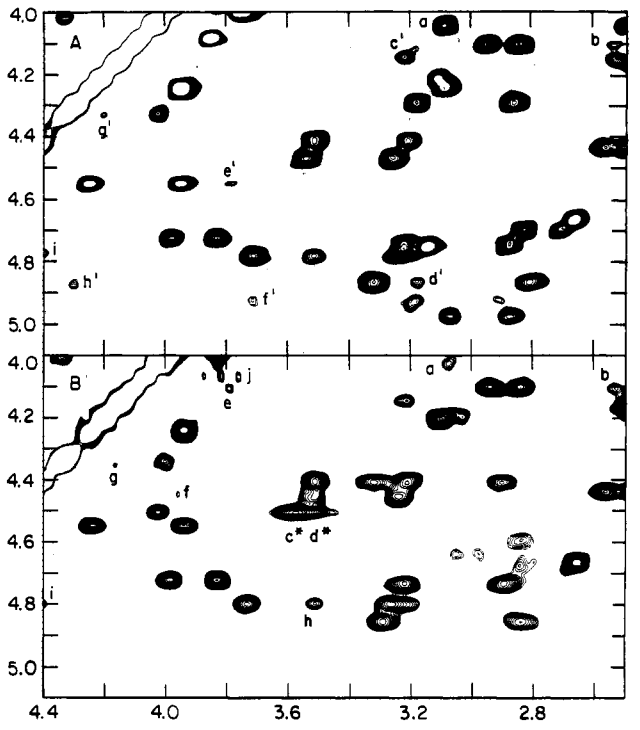

FIGURE 5: Spectrum showing sequential connectivities observed between ThrB27 and ProB28 in the NOESY spectrum of insulin (cross-peaks c and d in panel B; indicated by asterisks); as expected, these are absent in the NOESY spectrum of DPI (panel A). The remaining cross-peaks are similar in the two spectra. Assignments in panel A: (a) $B13H_\alpha$–$B16H_\beta$ and $B17H_\alpha$–$B16H_\beta$, (b) $A14H_\alpha$–$A17H_{\gamma 1}$, (c) $A16H_\alpha$–$A19H_{\beta 1}$, (d) $A6H_\alpha$–$A11H_\alpha$, (e) $A12H_\alpha$–$A13H_\alpha$, (f) $A7H_{\beta 1}$–$B7H_\alpha$, (g) $A4H_\alpha$–$A8H_\beta$, (h′) $A6H_\alpha$–$A10H_\alpha$, and (i) $A7H_\alpha$–$B5H_\alpha$. Assignments in panel B: (a) $B13H_\alpha$–$B16H_\beta$ and $B17H_\alpha$–$B13H_\beta$, (b) $A14H_\alpha$–$A17H_{\gamma 1}$, (c*) $B27H_\alpha$–$B28H_{\delta 1}$, (d*) $B27H_\alpha$–$B28H_{\delta 2}$, (e) $A13H_\alpha$–$A14H_\alpha$, (f) $A18H_\alpha$–$A15H_\alpha$, (g) $A4H_\alpha$–$A8H_\beta$, (h) $A7H_\alpha$–$B5H_{\beta 1}$, and (i) $B17H_\alpha$–$B16H_\alpha$. In each case the first assignment listed refers to the vertical frequency axis (ω_2) and the second is assigned to the horizontal frequency axis (ω_1). Intraresidue effects are not labeled. The mixing time was 200 ms. Axes are labeled in parts per million relative to acetic acid (2.03 ppm).

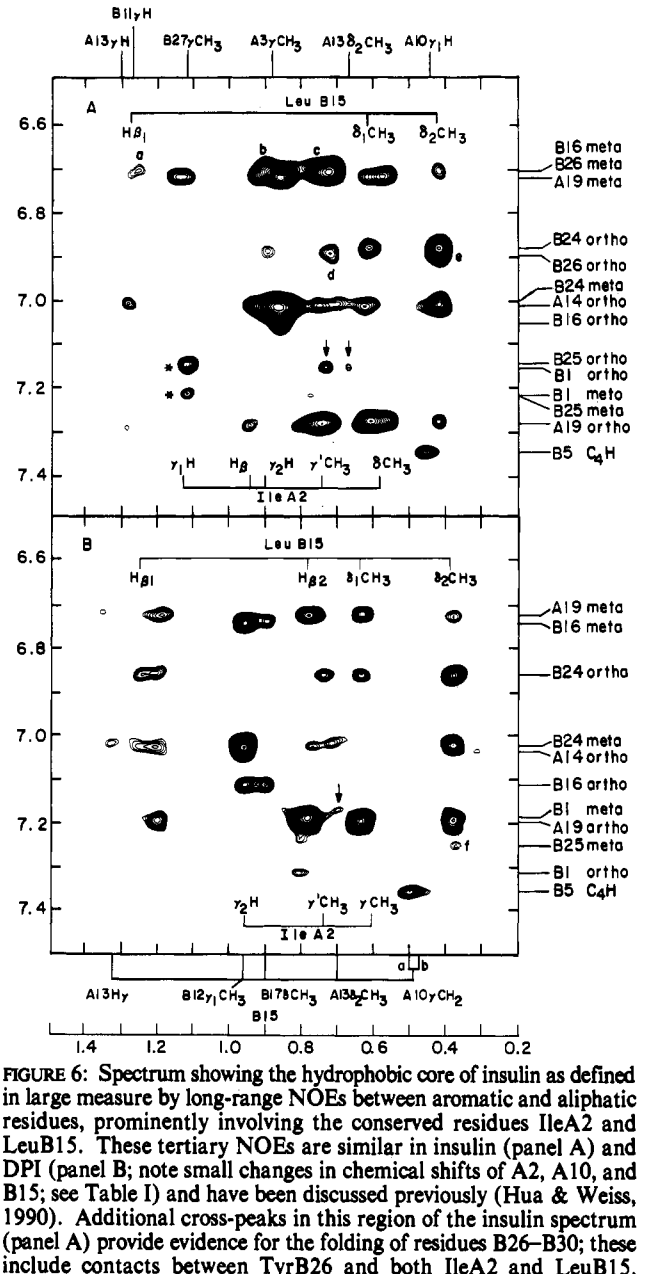

FIGURE 6: Spectrum showing the hydrophobic core of insulin as defined in large measure by long-range NOEs between aromatic and aliphatic residues, prominently involving the conserved residues IleA2 and LeuB15. These tertiary NOEs are similar in insulin (panel A) and DPI (panel B; note small changes in chemical shifts of A2, A10, and B15; see Table I) and have been discussed previously (Hua & Weiss, 1990). Additional cross-peaks in this region of the insulin spectrum (panel A) provide evidence for the folding of residues B26–B30; these include contacts between TyrB26 and both IleA2 and LeuB15. Asterisks in panel A indicate NOEs between the side chains of PheB25 and ThrB27 on the surface of the protein. Arrows in each panel represent NOEs between PheB1 and LeuA13. Additional assignments: (a) B26 meta–$B11H_\gamma$, (b) B26 meta–$A2H_{\gamma 2}$ and overlap with possible B12 and A3 NOEs, (c) B26 meta–$A2_\gamma CH_3$, (d) B26 ortho–$A2_\gamma CH_3$, (e) B26 ortho–$B15\delta_2CH_3$, and (f) B25 meta–$B15\delta_2CH_3$. In each case, the first assignment listed refers to the vertical frequency axis (ω_2), and the second is assigned to the horizontal frequency axis (ω_1). The mixing time was 200 ms. Axes are labeled in parts per million relative to acetic acid (2.03 ppm).

state); however, in molecule 2 of the 4-Zn hexamer (Dodson et al., 1979) and in the phenol-related hexamer (Derewenda et al., 1989), these residues are α-helical, forming an N-terminal extension of the central B-chain helix (the R state). In solution, no helix-related NOE or J-coupling patterns are observed (see Figure 4 and Table S4). The orientation of this region is in part determined by interchain NOEs between residues B3–B5 and IleA10; representative such NOEs ($B5H_\epsilon$–$A10_\gamma CH_3$ and $B5H_\epsilon$–$A10_\delta CH_3$) are shown in Figure 6. In crystals, HisB5 projects into a local pocket between the A- and B-chains, bordered in part by IleA10. Hydrogen bonds are also observed between chains in this region as discussed below (see Slowly Exchanging Amide Resonances and Dynamic Implications). Weak NOEs are observed between PheB1 and LeuA13 (arrows in panel A of Figure 6). Such NOEs are predicted by the 2-Zn structure of porcine insulin but not by the crystal structure of DPI (Bi et al., 1984; Dai et al., 1987). The relaxation properties of PheB1 suggest that it is flexible in solution (Wollmer et al., 1979; Weiss et al., 1989), and the observed NOE may reflect a transient excursion rather than a fixed distance. The general analysis of such situations is likely to require molecular dynamics simulation (Torda et al. 1990). This region of insulin is not thought to be involved in receptor binding (Pullen et al., 1976; Baker et al., 1988).

(iv) B-Chain β(1→4)-Turn and Residues B24–B30: Within the B-chain, residues B20–B23 form a β-turn, which has the effect of orienting PheB24 and TyrB26 back against the B-chain helix to pack against ValB12, PheB15, and TyrB16 (panel A of Figure 6; see also cross-peak m in panel A of Figure 4). These interactions define part of the hydrophobic core. In DPI, the B24 interactions are retained (panel B); its truncated B-chain ends with the disordered residue B25 (Hua & Weiss, 1990).

In crystal structures of insulin dimers, residues B25–B28 continue as a β-strand and pack against the underlying surface of the A-chain; residues B29 and B30 adopt variable or multiple positions (Baker et al., 1988; panel A of Figure 1). A key question concerns the relevance of this conformation to the solution structure of the monomer. Significant NOEs

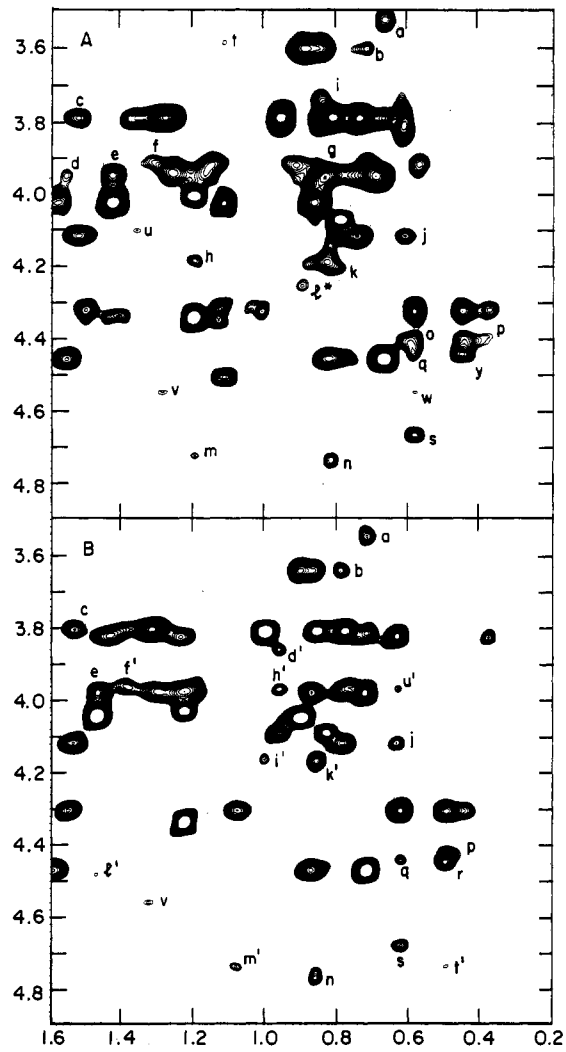

FIGURE 7: Spectrum showing the DPI moiety of intact insulin (panel A) and DPI itself (panel B) exhibiting a detailed correspondence or interresidue NOEs. A key cross-peak between ValA3 and ProB28 is observed in this region of the insulin spectrum (cross-peak 1 in panel A; indicated by asterisk); this long-range NOE tethers the C-terminal region of the B-chain to the underlying hydrophobic core. Other important interchain NOEs are observed in this region that are assigned to the DPI moiety of insulin; these include contacts between IleA2 and LeuB15 (which defines a helix–helix contact in the hydrophobic core) and between IleA10 and residues B3–B5 (which partially orients the N-terminal regions of the B-chain). Assignments in panel A: (a) $B5H_{\beta 1}$–$B6\delta_2CH_3$ and/or $B10H_{\beta 1}$–$B6\delta_2CH_3$, (b) $A3H_\alpha$–$A2_\gamma CH_3$, (c) $A13H_\alpha$–$A16H_{\beta 2}$, (d) $B11H_\alpha$–$B6H_\gamma$, (e) $B11H_\alpha$–$B14\beta CH_3$, (f) $A2H_\alpha$–$B15H_\gamma$, (g) $B11H_\alpha$–$B6\delta_{\gamma 1}CH_3$ and $B11H_\alpha$–$B6H_{\beta 2}$, (h) $A4H_\alpha$–$A8_\gamma CH_3$, (i) $A7H_{\beta 1}$–$A3\delta_2CH_3$, (j) $A16H_\alpha$–$B15\delta_1CH_3$, (k) $A4H_\alpha$–$A3_{\gamma 2}CH_3$, (l*) $B28H_\alpha$–$A3_{\gamma 1}CH_3$, (m) $A9H_\alpha$–$A8_\gamma CH_3$, (n) $B19H_\alpha$–$B18_{\gamma 2}CH_3$, (o) $B5H_\alpha$–$A10_\gamma CH_3$, (p) $B5H_\alpha$–$A10\delta CH_3$, (q) $B4H_\alpha$–$A10_\gamma CH_3$, (r) $B4H_\alpha$–$A10H_{\gamma 1}$, (s) $B3H_\alpha$–$A10_\gamma CH_3$, (t) $A3H_\alpha$–$A2H_{\gamma 1}$, (u) $A14H_\alpha$–$A13H_\gamma$, (v) $A12H_\alpha$–$A13H_{\beta 1}$, and (w) $A12H_\alpha$–$A10_\gamma CH_3$. Assignments in panel B: (a) $B10H_{\beta 1}$–$B6\delta_2CH_3$ (b′) $A3H_\alpha$–$B11\delta CH_3$, (c) $A13H_\alpha$–$A16H_{\beta 2}$, (d′) $B9H_{\beta 2}$–$B12_\gamma CH_3$, (e) $B11H_\alpha$–$B14\beta CH_3$, (f′) $A16H_\alpha$–$A13H_{\beta 2}$, (g) $B11H_\alpha$–$B6\delta_1CH_3$ and $B11H_\alpha$–$B6H_{\beta 2}$, (h′) $B11H_\alpha$–$B12_\gamma CH_3$, (i′) $A17H_\alpha$–$B18_{\gamma 1}CH_3$, (j) $A16H_\alpha$–$B15\delta_1CH_3$, (k′) $A17H_\alpha$–$B18_{\gamma 2}CH_3$, (l′) $B10H_\alpha$–$B14\beta CH_3$, (m′) $A9H_\alpha$–$A10\delta CH_3$ (n) $B19H_\alpha$–$B18_{\gamma 2}CH_3$, (o′) $B9H_\alpha$–$B12_\gamma CH_3$, (p) $B5H_\alpha$–$A10H_{\gamma 1}$, (q) $B4H_\alpha$–$A10_\gamma CH_3$, (r) $B4H_\alpha$–$A10H_{\gamma 1}$, (s) $B3H_\alpha$–$A10_\gamma CH_3$, (t′) $A9H_\alpha$–$A10H_{\gamma 1}$, (u′) $A12H_\alpha$–$A10_\gamma CH_3$, and (v′) $A12H_\alpha$–$A13H_\beta$. In each case the first assignment listed refers to the vertical frequency axis (ω_2) and the second is assigned to the horizontal frequency axis (ω_1). Intraresidue effects are not labeled. The mixing time was 200 ms. Axes are labeled in parts per million relative to acetic acid (2.03 ppm).

are observed between the B-chain β-strand and the A-chain that are in qualitative accord with the crystallographic dimer. Representative such NOEs between TyrB26 and IleA2 are shown in panel A of Figure 6 and between ProB28 and ValA3 in panel A of Figure 7 (asterisk). Nonlocal NOEs are not observed from residues B25, B27, and B29. The (i, i + 2, i + 4) pattern of contacts between residues B24–B26–B28 and the hydrophobic core suggests that the former region adopts an extended configuration, consistent with qualitative analysis of sequential and medium-range NOE patterns (Figure 3; see above).

No significant interresidue NOEs are observed involving LysB29 or ThrB30; these residues are likely to be disordered in acidic solutions. NOEs are also not observed between PheB25 and TyrA19, suggesting that the configuration of B25 is outward (molecule 2 in Chinese nomenclature) rather than inward (molecule 1). The relative absence of efficient cross-relaxation pathways (e.g., relative to internal rings TyrA19 or PheB24) suggests that the B25 ring may also be partly disordered as previously discussed (Weiss et al., 1989). Prominent (i, i + 2) NOEs between the B25 ring are observed with ThrB27 (asterisks in panel A of Figure 6) in accord with an outward orientation; only weak such effects would be predicted by an inward configuration (molecule 1 in Chinese nomenclature). The orientation of PheB25 may have implications for receptor recognition (Dodson et al., 1979; Nakagawa & Tager, 1986, 1987; Baker et al., 1988; Mirmira & Tager, 1989) and is addressed further in the Discussion in relation to the complementary studies of Boelens et al. (1990).

(v) *Disulfide bridges* provide covalent restraints between A6 and A11, A7 and B7, and A20 and B19 (Figure 1). In selected cases, nonlocal NOEs are also observed relating these cysteines, as discussed previously for DPI (Hua & Weis, 1990) and extended to insulin in the supplementary material.

Slowly Exchanging Amides and Dynamic Implications: Several slowly exchanging H_N resonances are observed in the spectrum of human insulin in freshly prepared D_2O solution, reflecting the presence of stable structure. Complete exchange requires 18–24 h at 25 °C, as shown in Figure 1S. This time course is essentially identical with that of DPI under the same conditions (Figure 11 of Hua and Weiss (1990)) and similar to that of insulin in 35% acetonitrile (Kline & Justice, 1990). The assigned resonances map to the B-chain helix (B10, B13–B19; however, B11 and B12 are unresolved in the aromatic region and may not be evaluated in 10 spectra), the N-terminal α-helix of the A-chain (A3 and A4), and the N-terminal portion of the second A-chain helix (residues A14–A17). In addition, slow exchange in observed among nonhelical residues IleA10, CysA11, LeuB6, and PheB24. Exchange of A11 and B6 is more rapid than the other sites (within 10 min), and similarly, "rapid" slow exchange of GlnB4 cannot be excluded due to partial overlap of resonances. Interestingly, the slowly exchanging subset of amide resonances includes many that are conformationally broadened. This correspondence suggests that the millisecond motions involved in the mechanism of broadening do not require the breakage of hydrogen bonds, including those involved in α-helix formation.

The similar exchange properties of insulin and DPI demonstrate that the addition of residues B26–B30 does not result in either global stabilization of the domain or local stabilization of the underlying N-terminal α-helix of the A-chain (panel A of Figure 1). This suggests that the C-terminal β-strand is not rigidly tethered to the hydrophobic core, a hypothesis that was previously motivated by observations of marked differences in the properties of native insulin and a single-chain analogue containing a peptide bond between LysB29 and GlyA1 (Markussen, 1985a,b; Weiss et al., 1989).

How can the slow exchange of nonhelical residues be explained? In crystal structures, the A11-NH and B6-NH groups are notable for participating in interchain hydrogen bonds (A11–B4 and B6–A3, respectively). Their protection, taken together with corroborative nonlocal NOEs (e.g., A6–B6, A7–B5, A7–B6, A10–B3, A10–B4, and A10–B5; see above), suggests that these hydrogen bonds are maintained in solution. The side chains of A10 and B24 also participate in interchain interactions (see above), but the hydrogen-bonding environments of their NH groups are presently unclear. In crystals, the A10-NH is variably positioned to form a hydrogen bond either to the carbonyl or side chain –OH of SerA5; the B24-NH is involved in a dimer-related β-sheet, which would not be relevant to the solution monomer (Baker et al., 1988). The presence of tertiary hydrogen bonds may be further explored following distance geometry/simulated annealing reconstruction of the solution structure (Wuthrich, 1990).

Discussion

This paper presents comparative 2D NMR studies of native human insulin and des-pentapeptide(B26–B30) insulin (DPI), an analogue lacking the five C-terminal residues of the B-chain (Gattner, 1975; Danho et al., 1975; Wang & Tsou, 1986). NMR characterization of these proteins is of interest in relation to protein dynamics and proposed mechanisms of conformational change. Crystal structures of insulin and insulin analogues are remarkable for differences in subunit conformation (Baker et al., 1988). Although an overall "insulin fold" may be defined, rigid body displacements of elements of secondary structure are seen, which require correlated changes in the configurations of multiple side chains. Such correlated motions have been investigated by thermal diffuse X-ray scattering studies of insulin crystals (Caspar et al., 1988) and by molecular dynamics simulations (Kruger et al., 1987; Caves et al., 1990). The existence of conformational substates in the insulin monomer, as inferred from solution NMR spectra, has previously been emphasized (Weiss et al., 1989, 1990; Kline & Justice, 1990; Boelens et al., 1990). To our knowledge, this paper describes the first detailed analysis of a protein NMR spectrum under conditions of extensive conformational broadening. Such an analysis is made possible in the present case by comparative study of an analogue (DPI) with more tractable spectroscopic properties (Figure 4).

Comparison of Insulin and DPI: For the purposes of NMR study, removal of residues B26–B30 results in significant improvement in the quality of the 2D data. This observation is of practical importance, since DPI appears to provide an appropriate NMR model for the solution structure of the corresponding portion of insulin, as indicated by a detailed similarity in their chemical shifts and NOE patterns. Insulin and DPI have previously been shown to adopt a similar conformation in the crystal state (Blundell et al., 1971; Peking Insulin Structure Group, 1971; Bi et al., 1984; Dai et al., 1987). Comparative analysis of insulin and DPI is seen to clarify potential ambiguities in sequential assignment otherwise associated with conformational broadening of amide resonances (Weiss et al., 1989; Kline & Justice, 1990). In the present study, this has made possible a complete assignment of the insulin spectrum. The interesting difference between insulin and DPI in the extent of resonance broadening is likely to have a dynamic mechanism: although corresponding protons experience similar *average* local environments in the two proteins (i.e., similar chemical shifts), more rapid motions in the fragment presumably lead to more complete averaging of chemical shifts on the NMR time scale (i.e., sharper cross-peaks for DPI). The nonlocal pattern of conformational broadening in each protein suggests that these motions are collective and involve all three α-helices. The presence of broad but slowly exchanging amide resonances further suggests that breakage of hydrogen bonds is not involved in these motions. Such features are in accord with a model of correlated displacements of units of secondary structure, as inferred from an analysis of structural differences among insulin crystal structures (Chothia et al., 1983). Such a mechanism may also account for the selective absence of long-range NOEs involving tertiary contacts that differ among crystal models. We speculate that the ensemble of solution structures spans the range of different crystal forms. The solution ensemble should exhibit the following general features.

(*i*) *Structural Features of the DPI Moiety*: The observed NMR features are in qualitative accord with overall features of the crystal structures of insulin and the crystal structure of DPI (Bi et al., 1984; Dai et al., 1987). In particular, the A-chain maintains a bent helix–loop–helix structure, with prominent NOEs observed among conserved residues at each end. The B-chain retains a central α-helix, followed by a β-turn. The N-terminal region is extended, and there is no evidence of helix formation as in variant crystal forms (the R state; Dodson et al., 1979; Derewenda et al., 1989). Interchain NOEs are observed that orient the three segments of α-helix; these are also in accord with crystal models. We emphasize, however, that various T-state crystal forms differ in the exact orientation of the α-helices; the present NMR results are not sufficiently precise to specify which of these crystal forms is most significantly populated in solution.

(*ii*) *Residues B24–B30*: The C-terminal region of the B-chain exists primarily as an extended strand and maintains contact with the underlying hydrophobic core (IleA2 and ValA3). This orientation has not previously been observed in an insulin monomer and has been the subject of considerable speculation in relation to the mechanism of insulin action (Dodson et al., 1979; Nakagawa & Tager, 1986, 1987; Baker et al., 1988; Mirmira & Tager, 1989). PheB25 appears to be largely flexible in solution and is discussed further below. No interresidue NOEs are observed from B29 and B30.

Relationship to Previous Studies: The present comparative study of human insulin and DPI may be compared with complementary 2D NMR approaches by other laboratories (Boelens et al., 1990; Kline & Justice, 1990). These studies exhibit important similarities and differences and are discussed in turn.

(*i*) *DPI in Aqueous Solution*: Kaptein and colleagues have recently reported the sequential assignment of the DPI monomer at pH 1.8 in aqueous solution (Boelens et al., 1990). Insulin cannot be studied under such conditions, since formation of dimers and high-order oligomers is observed as the concentration of deuterated acetic acid is reduced from 20 to 0% at pH 1.8–3.0 (Weiss et al., 1989). The difference in aggregation behavior between DPI and insulin is due to destabilization of the dimer interface following removal of residues B26–B30, which in the intact protein contribute to the intersubunit β-sheet and hydrophobic contacts between promoters (Baker et al., 1988).

The chemical shift values obtained in aqueous solution are in close accord with those observed in 20% acetic acid (Hua & Weiss, 1990), providing a detailed control for the absence of solvent perturbations in the present study. The studies differ, however, as follows. (a) Boelens et al. (1990) report the absence of slowly exchanging amide resonances in freshly prepared D_2O solutions, whereas a significant set of such resonances is observed in 20% acetic acid. This is an important

difference, as the presence (or absence) of slowly exchanging amide resonances provides evidence for the stability (or instability) of elements of secondary structure and the hydrophobic core. We have recently repeated our DPI studies under the conditions of Boelens et al. (1990) and observe a similar pattern of slowly exchanging amide resonances as in 20% acetic acid (Hua & Weiss, 1991). We cannot account for this discrepancy. (b) Boelens et al. (1990) describe a weak NOE between the meta resonance of PheB25 and an α-resonance of TyrA19 and conclude on this basis that PheB25 adopts an inward configuration in accord with molecule 1 of the 2-Zn structure (Chinese nomenclature). This NOE is not observed in 20% acetic acid. Accordingly, the present and related studies (Weiss et al., 1989, 1990; Hua & Weiss, 1990) support the opposite conclusion, i.e., that PheB25 is flexible and primarily adopts an outward configuration (molecule 2 of the 2-Zn structure). The relaxation properties of PheB25 suggest that this side chain is flexible, a result that is in accord with the crystal structure of DPI (Bi et al., 1984; Dai et al., 1987). The differences between the two studies may reflect the difference in solvent conditions (i.e., aqueous or 20% acetic acid). Alternatively, the existence of weak nonlocal NOEs may reflect in this case the transient excursion of a flexible side chain (B25) near a stably folded side chain (A19) rather than a fixed (but distant) contact. This point is of potential interest in relation to the mechanism of insulin action, since the two models differ in the exposure of PheB25 along the putative receptor-binding surface (Pullen et al., 1976; Baker et al., 1988). In the future, the differing interpretations of the two laboratories may be resolved by ^{13}C relaxation and isotope-editing NMR studies of DPI under various solution conditions and by complementary molecular dynamics simulations (Torda et al., 1990). We note that PheB25 appears to be flexible in an engineered insulin monomer under physiological conditions (Weiss et al., 1991).

(*ii*) *Native Insulin in an Organic Milieu*: Kline and Justice (1990) have recently described the sequential assignment of human insulin in 35% acetonitrile (pH 3.6). Similarities and differences are observed in two sets of chemical shifts (Table S3); the differences are most apparent among amide protons and presumably reflect direct and indirect (i.e., structural) effects of solvent composition. Use of a higher concentration of an organic cosolvent results in sharper resonances; this effect may be due to a dynamic mechanism analogous to that proposed in the case of DPI: more efficient averaging of chemical shifts following partial destabilization of the hydrophobic core. Such a mechanism is suggested by (i) a trend toward decreasing chemical shift dispersion in the spectrum of insulin with increasing concentrations of acetonitrile and (ii) observations that DPI is partially unfolded under these conditions (unpublished results). However, observation of α-helix-related NOE patterns in the A- and B-chains and corresponding slowly exchanging amide resonances demonstrates that ordered structure is retained in this more organic milieu.

Sequential contacts in this study were found unexpectedly to exhibit anomalies in the C-terminal region of the B-chain. The observed pattern—moderate d_{NN} connectivities, weak or absent $d_{\alpha N}$ connectivities—is inconsistent with the existence of a stably folded β-strand. We speculate that under these solvent conditions the insulin monomer undergoes a change in conformation relative to the crystallographic dimer (Kline & Justice, 1990). One possibility is that in 35% acetonitrile the C-terminal region of the B-chain is not tethered to hydrophobic core (as in the present study) but instead exists as multiple conformations in equilibrium. This hypothesis is consistent with the reported cis–trans isomerization of the ThrB27–ProB28 peptide bond; such isomerization is not detected in the present study. Long-range NOEs, such as those predicted to occur between this region and the A-chain, were not analyzed in the previous study (Kline & Justice, 1990). Further comparison of the structure of insulin under different solvent conditions will be of intrinsic interest and may complement our understanding of alternative subunit conformations observed in different crystal forms (Blundell et al., 1971; Dodson et al., 1979; Chothia et al., 1983). The relevance of these forms to the mechanism of insulin action has not been determined and may in the future be investigated by NMR studies of engineered insulin monomers under physiological conditions (Roy et al., 1990; Weiss et al., 1991).

Conclusions

Sequential ^1H NMR assignment of human insulin is accomplished by comparative analysis of the spectra of intact insulin and des-pentapeptide(B26–B30) insulin (DPI). The latter fragment has been previously analyzed (Boelens et al., 1990; Hua & Weiss, 1990) and provides an NMR model of the related portion of the intact protein. This correspondence enables potential ambiguities due to conformational broadening of amide resonances to be resolved. The following results are obtained. (1) The insulin monomer exists as a compact and stably folded domain in 20% acetic acid, as previously inferred from an analysis of aromatic ring resonances and photo-CIDNP enhancements (Weiss et al., 1989). (2) Insulin and DPI exhibit similar conformations under these conditions, in accord with their respective crystal structures. In particular, the N- and C-terminal α-helices of the A-chain and central α-helix of the B-chain are retained in both proteins and maintain analogous interchain contacts. (3) Slowly exchanging amide resonances are observed in both proteins, suggesting that elements of structure are stably maintained on the time scale of hours. This result is not in accord with a previous study (Boelens et al., 1990). (4) Differences are observed between DPI and insulin in the extent of conformational broadening, indicating that the presence or absence of residues B26–B30 influences the overall dynamics of the protein. The pattern of amide broadening and its solvent-exchange features suggest the existence of collective displacements of elements of secondary structure on a millisecond time scale. (5) The C-terminal region of the B-chain adopts an extended conformation (β-strand) and maintains close contact with the underlying hydrophobic surface of the A-chain. Anomalies observed in the NMR features of this region described in a more organic milieu (35% acetonitrile; Kline & Justice, 1990) are not observed in the present study, suggesting that in the earlier study the structure of insulin was influenced by solvent conditions. The present results support a model of collective millisecond motions in a protein and provide a foundation for their further characterization by distance geometry/simulated annealing methods.

Acknowledgments

We thank L. J. Neuringer (MIT) for continued encouragement and a critical reading of the manuscript; R. E. Chance and B. F. Frank (Eli Lilly & Co.) for DPI and biosynthetic human insulin; D. J. Patel (Columbia College of Physicians and Surgeons) for the seminal suggestion, based on studies of the bacteriophage P22 Arc repressor by his laboratory, of assigning the 2D NMR spectrum of a native protein by means of a more tractable analogue; J. Avruch, T. E. Blundell, P. DeMeyts, G. G. Dodson, M. Kochoyan, D. Nguyen, and S. E. Shoelson for helpful discussion; J. P. Lee for assistance with

NMR measurements; and Jai Wen-hua for assistance with NMR processing. The Harvard NMR Center was funded by a National Institutes of Health shared instrumentation grant (1 S10 RR04862-01) and an award from the National Health Resources Foundation. M.A.W. thanks Professors M. Karplus, C. T. Walsh, E. Blout, E. Braunwald, and J. T. Potts, Jr. for their encouragement.

Supplementary Material Available

Figure S1, demonstrating the time course of solvent exchange of amide resonances; Table S1, giving the stereospecific assignment of selected β resonances; Tables S2 and S3, listing the chemical shift differences between insulin and DPI and between human insulin in 20% acetic acid and 35% acetonitrile; Tables S4 and S5, showing apparent J-coupling constants for DPI and insulin, respectively; and a supplemental discussion concerning conformational broadening of amide resonances, interpretation of apparent coupling constants, and disulfide-related NOEs (15 pages). Ordering information is given on any current masthead page.

Registry No. Insulin, 11061-68-0; insulin monomer, 98743-24-9; despentapeptide (B26–B30) insulin, 55599-09-2.

References

Adams, M. J., Blundell, T. L., Dodson, E. J., Dodson, G. G., Vijayan, M., Baker, E. N., Hardine, M. M., Hodgkin, D. C., Rimer, B., & Sheet, S. (1969) *Nature (London) 224*, 491–495.

Badger, J. (1986) Ph.D. Thesis, University of York, York, England.

Baker, E. N., Blundell, T. L., Cutfield, G. S., Cutfield, S. M., Dodson, E. J., Boelens, R., Ganadu, M. L., Verheyden, P., & Kaptein, R. (1990) *Eur. J. Biochem. 191*, 147–153.

Dodson, G. G., Hodgkin, D. M. C., Hubbard, R. E., Iassac, M. W., Reynolds, D. C., Bentley, G., Dodson, E., Dodson, G., Hodgkin, D., & Mercola, D. (1976) *Nature (London) 261*, 166–168.

Bi, R. C., Dauter, Z., Dodson, E., Dodson, G., Giordano, F., & Reynolds, C. (1984) *Biopolymers 23*, 391–395.

Blundell, T. L., & Humbel, R. E. (1980) *Nature (London) 287*, 781–787.

Blundell, T. L., Cutfield, J. F., Cutfield, S. M., Dodson, E. J., Dondson, G. G., Hodgkin, D. C., Mercola, D. A., & Vijayan, M. (1971) *Nature (London) 231*, 506–511.

Casareto, M., Spoden, M., Diaconescu, C., Gattner, H.-G., Zahn, H., Brandenburg, D., & Wollmer, A. (1987) *Biol. Chem. Hoppe-Seyler 368*, 709–716.

Caspar, D. L. D., Clarage, J., Salunke, D. M., & Clarage, M. (1988) *Nature (London) 332*, 659–662.

Caves, L. S. D., Nguyen, D. T., & Hubbard, R. E. (1990) Conformation Variability of Insulin: A Molecular Dynamics Analysis in *Molecular Dynamics: An Overview of Applications in Molecular Biology* (Goodfellow, J. M., Ed.) pp 27–68, MacMillan Press, New York.

Chothia, C., Lesk, A. M., Dodson, G. G., & Hodgkin, D. C., (1983) *Nature (London) 302*, 500–505.

Dai, J.-B., Lou, M.-Z., You, J.-M., & Liang, D.-C. (1987) *Sci. China 30*, 55–65.

Danho, W. O., Gattner, H.-G., Nissen, D., & Zarn, H. (1975) *Hoppe-Seyler's Z. Physiol. Chem. 356*, 1406–1412.

Derewenda, U., Derewenda, Z., Dodson, E. J., Dodson, G. G., Reynolds, C. D., Smith, G. D., Sparks, C., & Swenson, D. (1989) *Nature (London) 338*, 594–596.

Dodson, E. J., Dodson, G. G., & Hodgkin, D. C. (1979) *Can. J. Biochem. 57*, 469–479.

Fischer, W. H., Saunders, D., Brandenburg, D., Wollmer, A., & Zahn, H. (1985) *Biol. Chem. Hoppe-Seyler 366*, 521–525.

Gattner, H. G. (1975) *Hoppe-Seyler's Z. Physiol. Chem. 356*, 1397–1404.

Haneda, M., Polonsky, K. S., Bergenstal, R. M., Jaspan, J. B., Shoelson, S. E., Blix, P. M., Chan, S. J., Kwok, S. C. M., Wishner, W. B., Zeidler, A., Olefsky, J. M., Freidenberg, G., Tager, H. S., Steiner, D. F., & Rubenstein, A. H. (1984) *N. Engl. J. Med. 310*, 1288–1294.

Hua, Q. X., & Weiss, M. A. (1990) *Biochemistry 29*, 10545–10555.

Hua, Q. X. & Weiss, M. A. (1991) *Biochim. Biophys. Acta* (in press).

Kline, A. D., & Justice, R. M., Jr. (1990) *Biochemistry 29*, 2906–2913.

Kruger, P., Strassburger, W., Wollmer, A., van Gunsteren, W. F., & Dodson, G. G. (1987) *Eur. Biophys. J. 14*, 449–459.

Liang, D.-C., Stuart, D., Dai, J.-B., Todd, R., You, J.-M., & Luo, M.-Z. (1985) *Sci. China 28*, 472–484.

Lu, Z. X. (1981) *Sci. China 26*, 1566–1574.

Markussen, J. (1985a) *Int. J. Pept. Protein Res. 25*, 431–434.

Markussen, J. (1985b) *Int. J. Pept. Protein Res. 26*, 70–77.

Mirmira, R., & Tager, H. S. (1989) *J. Biol. Chem. 264*, 6349–6354.

Nakagawa, S. H., & Tager, H. S. (1986) *J. Biol. Chem. 261*, 7332–7341.

Nakagawa, S. H., & Tager, H. S. (1987) *J. Biol. Chem. 262*, 12040–12058.

Neuhaus, D., Wagner, G., Vasak, M., Kagi, J. H. R., & Wuthrich (1985) *Eur. J. Biochem. 151*, 257–273.

Odawara, M., Kadowaki, T., Yamamoto, R., Shibasaki, Y., Tobe, K., Accili, D., Bevins, C., Mikami, Y., Matsuura, N., Akanuma, Y., Takaku, F., Taylor, S. I., & Kasuga, M. (1989) *Science 245*, 66–68.

Pardi, A., Billeter, M., & Wuthrich, K. (1984) *J. Mol. Biol. 180*, 741–751.

Peking Insulin Structure Group (1971) *Peking Rev. 40*, 11–16.

Pullen, R. A., Lindsay, D. G., Wood, S. P., Tickle, I. J., Blundell, T. L., Wollmer, A., Krail, A., Brandenburg, D., Zahn, H., Gliemann, J., & Gammeltoft, S. (1976) *Nature (London) 259*, 369–373.

Reidhaar-Olson, J. F., & Sauer, R. T. (1988) *Science 241*, 53–57.

Roy, M., Lee, R. W.-K., Brange, J., & Dunn, M. F. (1990) *J. Biol. Chem. 265*, 5448–5454.

Smith, G. D., Swenson, D. C., Dodson, G. G., & Reynolds, C. D. (1984) *Proc. Natl. Acad. Sci. U.S.A. 81*, 7093–7097.

States, D. J., Haberkorn, R. A., & Ruben, D. J. (1982) *J. Magn. Reson. 48*, 286–292.

Taira, M., Taira, M., Hashimoto, N., Shimada, F., Suzuki, Y., Kanatsuka, A., Nakamura, F., Ebina, Y., Tatibana, M., Makino, H., & Yoshida, S. (1989) *Science 245*, 63–66.

Torda, A. E., Sheek, R. M., & van Gunsteren, W. F. (1990) *J. Mol. Biol. 14*, 223–235.

Wagner, G., Braun, W., Havel, F. T., Shaumann, T., Go, N., & Wuthrich, K. (1987) *J. Mol. Biol. 196*, 611–633.

Wang, C.-C., & Tsou, C.-L. (1986) *Biochemistry 25*, 5336–5340.

Weiss, M. A., Eliason, J. A., & States, D. J. (1984) *Proc. Natl. Acad. Sci. U.S.A. 81*, 6019–6023.

Weiss, M. A., Nguyen, D. T., Khait, I., Inouye, K., Frank, B. H., Beckage, M., O'Shea, E. K., Shoelson, S. E., Karplus, M., & Neuringer, L. J. (1989) *Biochemistry 28*, 9855–9873.

Weiss, M. A., Frank, B. H., Khait, I., Pekar, A., Heiney, R., Shoelson, S. E., & Neuringer, L. J. (1990) *Biochemistry 29*, 8389–8401.
Weiss, M. A., Hua, Q. X., Frank, B. H., & Shoelson, S. E. (1991) *Biochemistry* (in press).
Wollmer, A., Fleischhauer, J., Strassburger, W., Thiele, H., Bradenburg, D., Dodson, G., & Mercola, D. (1979) *Biophys. J. 20*, 233–243.
Wollmer, A., Strassburger, W., Glatter, U., Dodson, G. G., & McRittel, W. (1981) *Hoppe-Seyler's Z. Physiol. Chem. 362*, 581–591.
Wuthrich, K. (1986) *NMR of Proteins and Nucleic Acids*, John Wiley & Sons, New York.
Wuthrich, K. (1990) *Methods Enzymol. 177*, 125–131.
Wuthrich, K., Wider, G., Wagner, G., & Braun, W. (1983) *J. Magn. Reson. 55*, 311.

ESR Spectra Reflect Local and Global Mobility in a Short Spin-Labeled Peptide throughout the α-Helix → Coil Transition†

A. P. Todd and G. L. Millhauser*
Department of Chemistry and Biochemistry, University of California, Santa Cruz, California 95064
Received August 27, 1990; Revised Manuscript Received March 9, 1991

ABSTRACT: A series of short alanine-based synthetic peptides (16 or 17 residues) have previously been shown to exhibit an anomalously high degree of α-helicity [Marqusee, S., et al. (1989) *Proc. Natl. Acad. Sci. U.S.A. 86*, 5286–5290; Marqusee, S., & Baldwin, R. L. (1987) *Proc. Natl. Acad. Sci. U.S.A. 84*, 8898–8902]. These peptides are ideal models for extracting position-dependent structural and dynamic information. Using the methanethiosulfonate nitroxide spin label (MTSSL), we labeled an analogue of the salt-bridge-stabilized "i+4" peptide, called the "i+4c", which has a specific attachment site created by replacing the central alanine with a cysteine. Circular dichroism (CD) spectra demonstrate that the i+4c-MTSSL peptide retains nearly the same helicity as the original i+4 peptide. The ESR spectra of the labeled peptide indicate no significant aggregation. ESR spectra were acquired throughout the helix–coil transition by temperature variation. From the motionally narrowed spectra, we extracted the rotational correlation times of the nitroxide label. Parallel measurements with circular dichroism enabled us to relate these parameters directly to the fractional helicity. For comparison, we followed a similar procedure with MTSSL-labeled glutathione (GS-MTSSL), a tripeptide that does not form an α-helix. Our results are interpreted in terms of a local tumbling volume, V_L, which reflects the portion of the peptide that reorients with the nitroxide label. At high fractional helicity, V_L is similar to the volume expected for a 17-residue helix. Only when the fractional helicity is lowered below 40% does V_L decrease, thereby indicating the onset of segmental motion of the peptide backbone. We analyze these results in terms of both a cooperative and a noncooperative model of the α-helix → coil transition, and we propose that the simplest cooperative view is not complete. Our experimental results and analysis show that spin label ESR is an excellent tool for rapidly extracting important structural information from nanomole quantities of peptide.

The α-helix is the most common type of secondary structure found in proteins, and the formation of α-helix from the random coil is the most well-characterized folding transition. Nevertheless, the dynamics of the α-helix → coil transition remain poorly understood. For example, it is not known whether helix formation is all-or-none (highly cooperative) or develops in a graded manner (noncooperative) in short peptide molecules. Experimental results have come almost exclusively from long-chain homopolypeptides. Thus, little is known about the transition for heterooligomers in aqueous solution, which are more appropriate models for the folding of naturally occurring proteins. Zimm–Bragg (1959) theory, along with helix/coil parameters (σ and s) from host–guest studies (Sueki et al., 1984), suggests that short peptides (<20 residues) containing helix-forming amino acids will be just on the threshold of exhibiting measurable helical structure (Shoemaker et al., 1985).

Experimentally, short helical peptides do appear to be relatively rare although there are several examples beginning with the C- and S-peptide fragments of ribonuclease A (Brown & Klee, 1971). Recently, a series of 16- and 17-residue alanine-based peptides have been synthesized (Marqusee & Baldwin, 1987; Marqusee et al., 1989) and found to have a helical content of greater than 70% at 1.0 °C. The enhanced helical stability in these peptides results partly from position-dependent effects ignored by the Zimm–Bragg theory. However, it has been proposed that the more important contribution arises from a high helix/coil equilibrium constant (s value) for alanine, which was previously underestimated in host–guest studies (Marqusee et al., 1989). Such peptides afford the exciting opportunity of studying molecular structure and dynamics in short helical segments.

The most helical of this series of synthetic peptides is the "i+4(E,K)", which is a 17-mer with positively charged lysine residues at positions 6, 11, and 16, negatively charged glutamate residues at positions 2, 7, and 12, and alanine residues at all other positions. In addition to the high helical propensity for alanine, the helical form of this peptide is stabilized by charged group interactions with the helix dipole and by salt bridge formation between lysine and glutamate residues oc-

†This work was supported by a grant from the National Science Foundation (DMB-8916946). Portions of this work were also supported by faculty research funds granted by the University of California, Santa Cruz. Acknowledgement is made to the donors of the Petroleum Research Fund, administered by the American Chemical Society, for partial support of this research.

0006-2960/91/0430-5515$02.50/0